

Fast Microwave-Induced Thermoacoustic Tomography Based on Multi-Element Phase-Controlled Focus Technique *

ZENG Lü-Ming(曾吕明), XING Da(邢达)**, GU Huai-Min (谷怀民), YANG Di-Wu(杨迪武),
YANG Si-Hua(杨思华), XIANG Liang-Zhong(向良忠)

MOE Key Laboratory of Laser Life Science and Institute of Laser Life Science, South China Normal University,
Guangzhou 510631

(Received 28 December 2005)

We develop a fast microwave-induced thermoacoustic tomography system based on a 320-element phase-controlled focus linear transducer array. A 1.2-GHz microwave generator transmits microwave with a pulse width of $0.5 \mu\text{s}$ and an incident energy density of $0.45 \text{ mJ}/\text{cm}^2$, and the microwave energy is delivered by a rectangular waveguide with a cross section of $(80.01 \pm 0.02) \times 10^{-4} \text{ m}^2$. Compared to single transducer collection, the system with the multi-element linear transducer array can eliminate the mechanical rotation of the transducer, hence can effectively reduce the image blurring and improve the image resolution. Using a phase-controlled focus technique to collect thermoacoustic signals, the data need not be averaged because of a high signal-to-noise ratio, resulting in a total data acquisition time of less than 5 s. The system thus provides a rapid and reliable approach to thermoacoustic imaging, which can potentially be developed as a powerful diagnostic tool for early-stage breast caners.

PACS: 43.35.+d, 87.57.Ce, 43.60.+d, 43.80.+p

Microwave-induced thermoacoustic tomography (MITT) combines the merits of both pure ultrasonic and microwave imaging, and achieves excellent ultrasound spatial resolution and microwave absorption contrast.^[1,2] This hybrid technology has the potential to revolutionize ultrasonic and microwave imaging in small animals and human beings, when compared to competing techniques for diagnosis of breast cancer.

The basic idea of MITT is that when a sample is irradiated by a short pulse of microwave, the deposited energy may result in a sample expansion and subsequent contraction that generates time-dependent thermoacoustic waves.^[3] The microwave pulse is so short that the energy will convert into heat by fast non-irradiative relaxation processes.^[4] The penetration depth of microwave radiation can reach several centimetres in biological tissue, which is deeper than that of light.^[5-7] In recent years, MITT has become a popular research subject and been used in imaging of the energy-absorption patterns within biological tissues.^[8-10] In these experiments, a single ultrasonic transducer is used to detect thermoacoustic signals by rotating it around a sample for 360° . The experimental setups are mechanically complicated, which affects the reliability of the experimental measurement, and the relative long time for data acquisition hampers the practical application of MITT.

We have recently reported a multi-element linear transducer array system (MLTAS) for two-dimensional (2-D) tissue photoacoustic imaging.^[11-13] In the present work, we develop a fast MITT system with the MLTAS, which is composed of a signal preamplifier, a multiple way switch and

a phase adjusting circuit. Using the multi-element phase-controlled focus technique, we can reduce the total time of data acquisition within 5 s, and can improve the reliability and convenience of MITT. Here, we report initially the validation of our imaging system, and our ultimate aim is to diagnose early-stage breast caners.

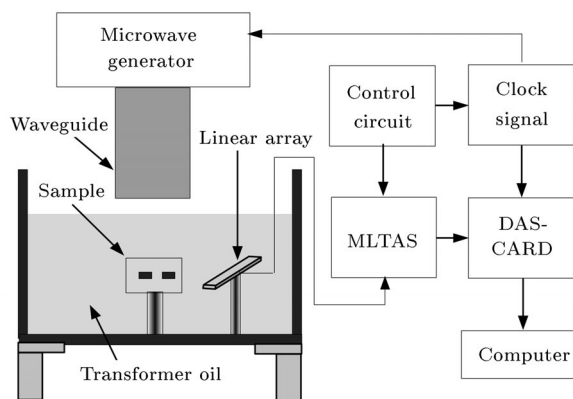


Fig. 1. Experimental setup for MITT.

The schematic of the experimental setup is shown in Fig. 1. A microwave generator (BW-1200HPT, China) provides 1.2-GHz microwave pulses for thermoacoustic auditory generation. The pulses have the following properties: pulse-duration of $0.5 \mu\text{s}$ and incident energy density of $0.45 \text{ mJ}/\text{cm}^2$. The microwave pulses are coupled into a rectangular waveguide with a cross section of $12.7 \text{ cm} \times 6.3 \text{ cm}$ and irradiated to a sample uniformly. The sample is placed on a plastic stage and immersed in a plexiglass tank, which is

* Supported by the National Natural Science Foundation of China under Grant Nos 60378043 and 30470494, and the Natural Science Foundation of Guangdong Province (015012; 04010394; 2004B10401011).

** To whom correspondence should be addressed. Email: xingda@sncu.edu.cn

filled with transformer oil for better coupling of acoustic waves.

In our experiment, a new B-mode system (Model CTS-200, SIUI, China) is modified as our platform with 320 vertical transducer elements (EZU-PL21). The transducer is divided into 64 sub-groups, and each sub-group consists of five transducer elements, which are selected with a custom-built control circuit. The transducer elements have a length of 10 mm, a width of 0.3 mm, a pitch of 0.04 mm and a thickness of 0.5 mm. The resonance frequency of the transducer is 3.5 MHz, and the scanning width is 102 mm. A built-in acoustic lens made from silicon rubber selects a 2-D image plane and suppresses out of plane signals. A two-channel DAS card (Compuscope 12100, Gage Applied Co., Montreal, Quebec, Canada) is used to recorded thermoacoustic signals. The card features a high-speed 12-bit analogue-to-digital converter with a sampling rate of 100 MHz. The system operation and data collection are controlled by a personal computer.

A clock signal, provided by the custom-built control circuit, is used for synchronized triggering the microwave generator and the data-acquisition system (DAS) card. With the multiway electronic switch of MLTAS, the custom-built control circuit selects eleven transducer elements of the linear transducer array to capture the induced thermoacoustic signals. The signals from the transducer elements, after pre-amplification and phase adjustment, are acquired with the DAS card without average. The EUZ-PL21 linear array is fixed on the right side and pointed to the centre of sample stage. We added some corrections to the multi-element phase-controlled focus algorithm for acoustic attenuation and nonideal focusing effect. Meanwhile, it would reduce the lateral resolution of our system slightly.^[14] The reconstructed image was amplified with an exponential gain compensation of up to 24 dB.

Consider a biological tissue irradiated by a short pulse microwave. When microwave absorption takes place, the thermoacoustic waves can be described by the following differential equation:^[6]

$$\nabla^2 p(\mathbf{r}, t) - \frac{1}{c^2} \frac{\partial^2 p(\mathbf{r}, t)}{\partial t^2} = -\frac{\beta}{C_p} \frac{\partial H(\mathbf{r}, t)}{\partial t}, \quad (1)$$

where β is the isobaric volume expansion coefficient, c is the speed of sound, c_p is the heat capacity, $p(\mathbf{r}, t)$ is the thermoacoustic pressure at position \mathbf{r} and time t , and $H(\mathbf{r}, t)$ is the heating function defined as the thermal energy per unit time and unit volume deposited by the energy source. Thermal confinement condition is assumed, where the acoustic transit time across the acoustic source is less than the heat conduction time. Equation (1) can be replaced under the zero-initial-value conditions $p(\mathbf{r}, 0) = 0$ and $(\partial/\partial t)p(\mathbf{r}, 0) = 0$

by^[6]

$$p(\mathbf{r}, t) = \frac{\beta}{4\pi C_p} \iiint \frac{d\mathbf{r}'}{|\mathbf{r} - \mathbf{r}'|} \left. \frac{\partial H(\mathbf{r}', t')}{\partial t'} \right|_{t'=t-\frac{|\mathbf{r}-\mathbf{r}'|}{c}}. \quad (2)$$

In fact, the transducer is not an ideal point detector. For simplicity, we can ignore its size if we put it far away from the sample. However, we still have to consider the impulse response function of the transducer and the temporal profile of the microwave pulse $s(t)$. Therefore, the system point spread function $R(\mathbf{r}_0, t)$ can be written as a convolution

$$R(\mathbf{r}_0, t) = p(\mathbf{r}_0, t) * i(\mathbf{r}_0, t) * s(t), \quad (3)$$

where $*$ denotes convolution, \mathbf{r}_0 denotes the position of an ideal point absorber, $R(\mathbf{r}_0, t)$ is the thermoacoustic pressure of the ideal point absorber induced by an ideal delta-pulse microwave pumping as shown in Fig. 2(a), and $i(\mathbf{r}_0, t)$ is the recorded photoacoustic signal from a point source, which is the convolution of induced photoacoustic pressure and impulse response of the transducer. It can be easily measured by focusing the incident laser on an absorber surface to form a point source. Because the propagation speed of electromagnetic wave is much greater than the speed of sound, the sample volume illuminated by microwave pulses radiates acoustic waves simultaneously.^[6] Figure 2(b) shows the temporal profile of the microwave pulse $s(t)$, which is a rectangular function with duration of 0.5 μ s. Figure 2(c) exhibits the experimentally measured piezoelectric output $i(\mathbf{r}_0, t)$, whose frequency spectrum is shown in Fig. 2(d). Theoretically, the measured signal $p'(\mathbf{r}, t)$ is the convolution of the thermoacoustic pressure and the system point spread function $R(\mathbf{r}_0, t)$, so we can compute $p(\mathbf{r}, t)$ by^[9]

$$p'(\mathbf{r}, t) = p(\mathbf{r}, t) * R(\mathbf{r}_0, t). \quad (4)$$

Then $p(\mathbf{r}, t)$ can be obtained by deconvoluting the piezoelectric output $R(\mathbf{r}_0, t)$ of the transducer in response to the measured thermoacoustic signal from a point source,^[15]

$$\frac{\partial p(\mathbf{r}, t)}{\partial t} \approx \text{IFFT} \left[\frac{j\omega p'(\omega)}{R(\omega)} \right] \left[1 + \cos \left(\frac{\pi\omega}{\omega_c} \right) \right], \quad (5)$$

where $p'(\omega)$ and $R(\omega)$ are the Fourier transform of the thermoacoustic signal $p'(\mathbf{r}, t)$ and the system point spread function $R(\mathbf{r}_0, t)$, respectively. The apodizing function $1 + \cos(\pi\omega/\omega_c)$ is the window function used to band-limit the signals to the cut-off frequency of ω_c .

In our experiments, the theoretical system point spread function deduced according to Eq. (3) is plotted in Fig. 2(e) as a dashed line, and the experimental one measured by illuminating a homogeneous pork fat tissue embedded with a gelatine spot with the linear transducer array is plotted in Fig. 2(e) as a solid line for comparison, where the slight offset is caused by

an oscilloscope in the experimental detection. From Fig. 2(e), we can see that the experimental and theoretical system point spread functions match well, which proves the feasibility of the indirect method to obtain the MITT system point spread functions, because photoacoustic transition as a thermoelastic effect is similar to microwave-induced thermoacoustic transition and the impulse response of the transducer

is difficult to be direct-measured exactly.^[15] The curvilinear oscillation of Fig. 2(e) is caused by a nonideal phase-controlled focus effect, which can reach approximately 91% of the ideal value. Figure 2(f) shows a frequency spectrum of the system point spread function, so we choose the cut-off frequency $\omega_c = 5$ MHz in the window function.

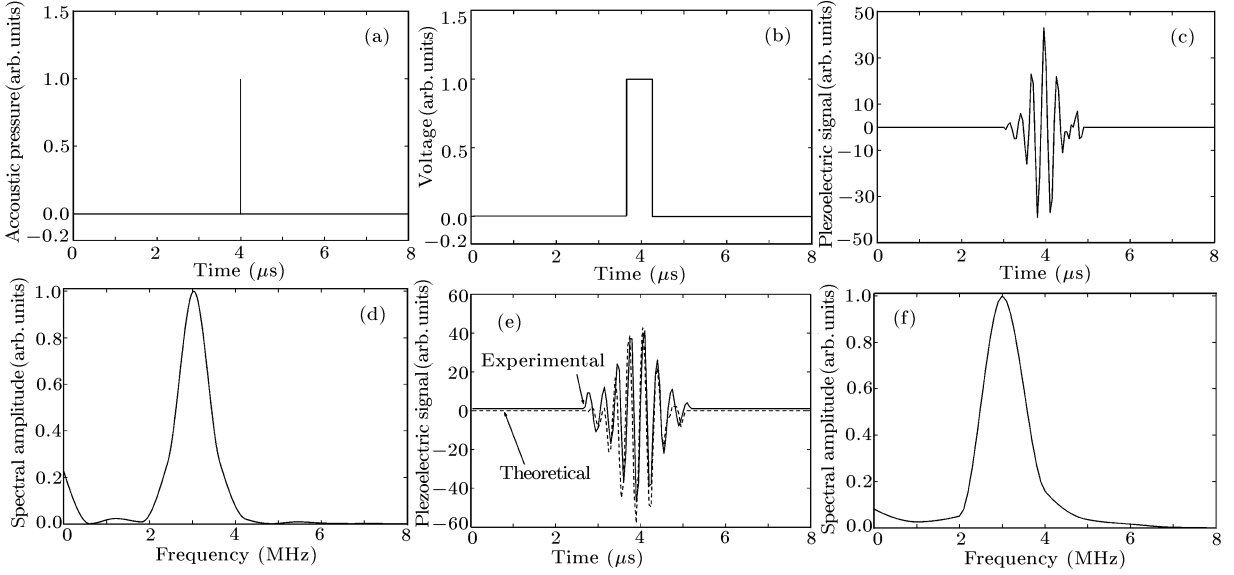


Fig. 2. (a) Thermoacoustic pressure of an ideal point absorber induced by an ideal delta-pulse microwave pumping. (b) Temporal profile of the microwave pulse. (c) Experimentally recorded photoacoustic signal from a point source with the linear transducer array. (d) Frequency spectrum of the recorded photoacoustic signal from a point source. (e) Experimental and theoretical system point spread functions of the transducer output. (f) Frequency spectrum of the system point spread function.

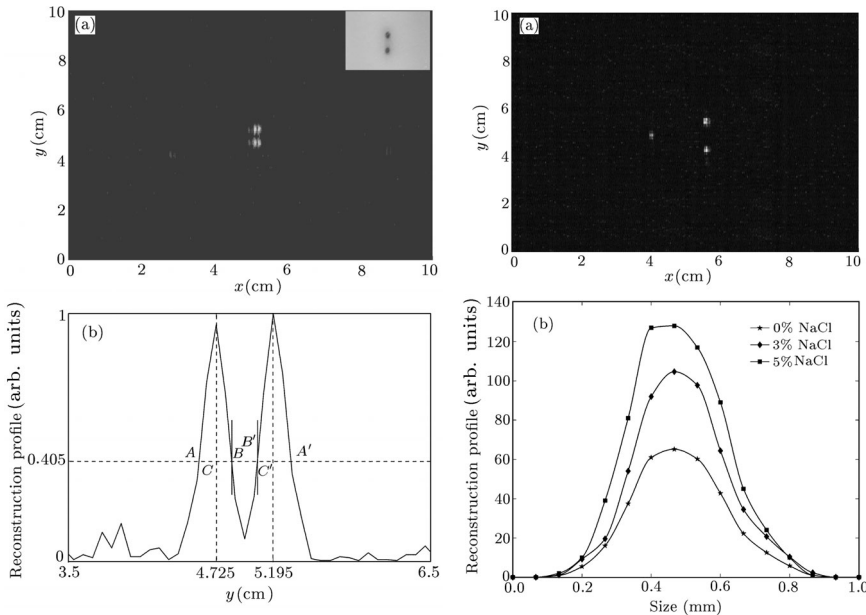


Fig. 3. (a) Thermoacoustic reconstructed image and a reduced cross section of the tissue sample and (b) the line profile of the reconstructed image (a) at $x = 5.23$ cm.

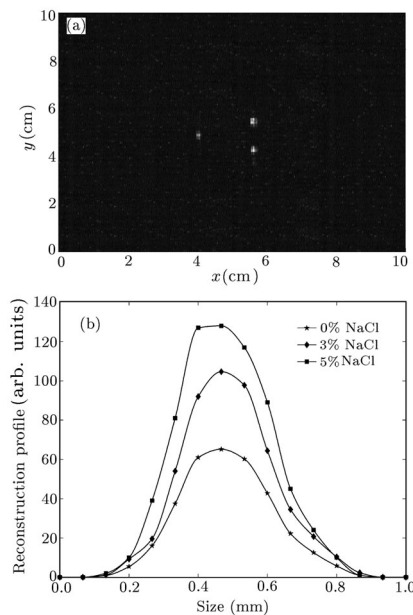


Fig. 4. (a) Thermoacoustic reconstructed image of the sample depending on different microwave absorption coefficients and (b) 1-D reconstruction profiles along the x axis.

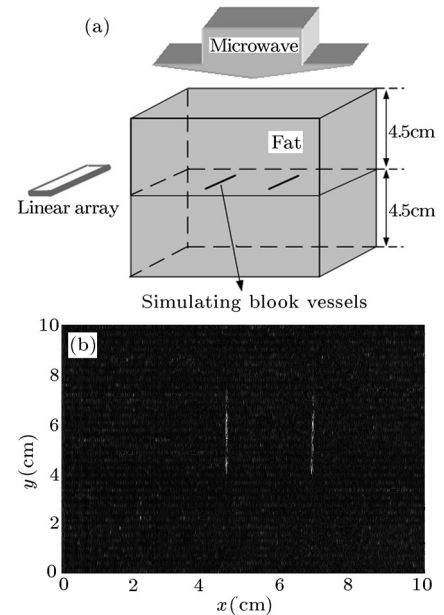


Fig. 5. (a) Diagram of the sample structure and the measurement and (b) thermoacoustic tomography image of the simulating blood vessels.

With a delay-circuit and multi-element phase-controlled focus technique, MLTAS detecting the thermoacoustic signals is similar to that used in photoacoustic imaging.^[12] Consider that a thermoacoustic source is outside the focal region, the signals from this particular point collected by the detectors are incoherent, so the amplitude of the signal after synthesizer is reduced due to phase cancellation. Therefore, multi-element phase-controlled focus technique can greatly improve the SNR of the thermoacoustic signals.

A sample with two small thermoacoustic sources was used to test the spatial resolution of our system. The sample was a piece of homogeneous pork fat tissue embedded with two gelatine spots, which were made of 12% gelatine, 85% water, 3% NaCl, and a drop of dark ink (to improve the photographic properties of the sample). Some NaCl would lead to an increase in the conductivity of microwave and result in an increased energy absorbed.^[2] In the frequency of 1.2 GHz, the relative permittivity of pork fat tissue has a value of approximately 3.2. The diameter of the gelatine spots is 2.1 mm, and the distance between them is 2.5 mm. Figure 3(a) shows the reduced physical dimensions of the test sample photograph before the experiment and the two-dimensional image produced by our phase-controlled reconstructed algorithm. The relative locations and fore-and-aft boundary of those small thermoacoustic sources are clearly resolved and perfectly match with the original sample. Figure 3(b) shows a reconstructed profile at position $x = 5.23$ cm of the image shown in Fig. 3(a). The profile includes the two absorption sources. The 40.5%-amplitude line intercepts with the profile at points A , B and A' , B' . It also cuts across the centrelines of the two absorption peaks at points C and C' . The distances of $|BC|$ and $|B'C'|$ are 1.29 mm and 1.30 mm, respectively. Therefore, the minimum distinguishable distance R between two sources is approximately $R = |BC| + |B'C'| - 2r$, where r is the radius of the absorption source. From Fig. 3(b), the distance R , which is the spatial resolution of our imaging system, is determined to be 0.5 mm.

In order to study the dependence of the acoustic pressure on the microwave absorption coefficient, we choose three point absorbers which are made of the same amount of gelatine (12%) and different amounts of NaCl (0%, 3%, and 5%). Figure 4(a) shows the thermoacoustic reconstructed image of the sample. The one-dimensional fitted reconstruction profiles of the three point absorbers along the x axis are combined, as shown in Fig. 4(b). It can be seen that the amplitudes of the reconstruction profiles increase with the increasing ionic concentration, because an increase of the dielectric constant results in an energy increase of the absorbers. The growth of any cancerous tissue depends on its ability to maintain a nutrient supplied by the delivering of mass blood vessels, which

are abundant in blood and ions leading to a good microwave energy absorption coefficient. Therefore, MITT of stimulating blood vessels as well as blood vessels can be potentially developed to detect early-stage cancers.

The advantage of using microwave is its good penetration depth in soft tissue. A microwave can reach a deep tumour embedded in tissue and irradiate it to generate thermoacoustic waves. Figure 5(a) shows a diagram of the sample structure and the measurement. The sample was made according to the following procedure. We made a piece of quadrate homogeneous pork fat tissue with a thickness of 4.5 cm. Next, we placed parallel two simulating blood vessels on the fat tissue. The simulating blood vessels were made of silicon rubber tubes with 0.8 mm diameter, filled with chicken blood. The length of the blood vessels and the distance between them are 3.1 cm and 2.3 cm, respectively. Then we cover the simulating blood vessels with the same thickness fat tissue. In order to finalize the design, the sample was cooled at room temperature for several minutes. Figure 5(b) shows the thermoacoustic tomography image of the simulating blood vessels with phase-controlled focus reconstructed algorithm. From the reconstructed image, the image of simulating blood vessels is in excellent agreement with the real sample. However, the background noise of the reconstructed image is not as well as that of the images, because the thick fat tissue results in an attenuation of thermoacoustic signal intensity and microwave energy.

References

- [1] Kruger R A, Kopecky K K, Aisen A M *et al* 1999 *Radiology* **211** 275
- [2] Wang L H, Zhao X, Sun H and Ku G 1999 *Rev. Sci. Instrum.* **70** 3744
- [3] Kruger R A, Reinecke D R and Kruger G A 1999 *Med. Phys.* **26** 1832
- [4] Xu M H and Wang L H 2002 *Med. Phys.* **29** 1661
- [5] Su Y, Zhang F, Xu K, Yao J and Wang R K 2005 *J. Phys. D: Appl. Phys.* **38** 2640
- [6] Han Q B, Wang H and Qing M L 2005 *Chin. Phys. Lett.* **22** 3104
- [7] Hu W X and Xie B S 2004 *Chin. Phys. Lett.* **21** 1294
- [8] Ku G and Wang L H 2000 *Med. Phys.* **27** 1195
- [9] Xu M H and Wang L H 2002 *IEEE Trans. Med. Imaging* **21** 814
- [10] Kruger R A, Kiser W L, Miller K D and Reynolds H E 2000 *Proc. SPIE* **3916** 150
- [11] Zeng Y G, Xing D, Wang Y, Yin B Z and Chen Q 2004 *Opt. Lett.* **29** 1760
- [12] Yin B Z, Xing D, Wang Y, Zeng Y G, Tan Y and Chen Q 2004 *Phys. Med. Biol.* **49** 1339
- [13] Yang D W, Xing D, Gu H M, Tan Y and Zeng L M 2005 *Appl. Phys. Lett.* **87** 194101
- [14] Niederhauser J J, Jaeger M, Lemor R, Weter P and Frenz M 2005 *IEEE Trans. Med. Imaging* **24** 436
- [15] Wang Y, Xing D, Zeng Y G and Chen Q 2004 *Phys. Med. Biol.* **49** 3117